Filler characteristics of modern dental resin composites and their influence on physico-mechanical properties

Randolph , Luc D; Palin, William; Leloup, Gaetane; Leprince, Julian G

DOI:
10.1016/j.dental.2016.09.034

Document Version
Peer reviewed version

Citation for published version (Harvard):
Randolph , LD, Palin, W, Leloup, G & Leprince, JG 2016, 'Filler characteristics of modern dental resin composites and their influence on physico-mechanical properties', *Dental Materials*, vol. 32, no. 12, pp. 1586-1599. https://doi.org/10.1016/j.dental.2016.09.034

Title: Filler characteristics of modern dental resin composites and their influence on physicomechanical properties

Author: Luc D. Randolph William M. Palin Gaëtane Leloup Julian G. Leprince

PII: S0109-5641(16)30461-4
DOI: http://dx.doi.org/doi:10.1016/j.dental.2016.09.034
Reference: DENTAL 2850

To appear in: *Dental Materials*

Received date: 8-5-2016
Revised date: 15-9-2016
Accepted date: 22-9-2016

Please cite this article as: Randolph Luc D, Palin William M, Leloup Gaëtane, Leprince Julian G.Filler characteristics of modern dental resin composites and their influence on physicomechanical properties.*Dental Materials* http://dx.doi.org/10.1016/j.dental.2016.09.034

Filler characteristics of modern dental resin composites and their influence on physicomechanical properties

Luc D. Randolph[a,b,c*], William M. Palin[d], Gaëtane Leloup[a,b,c,e], Julian G. Leprince[a,b,c,e]

Authors' adressess

[a] ADDB, Louvain Drug Research Institute, Université catholique de Louvain, Brussels, Belgium

[b] Institute of Condensed Matter and Nanosciences, Bio- and Soft- Matter, Université catholique de Louvain, Louvain-la-Neuve, Belgium

[c] CRIBIO (Center for Research and Engineering on Biomaterials), Brussels, Belgium

[d] Biomaterials Unit, University of Birmingham, College of Medical and Dental Sciences, School of Dentistry, St Chad's Queensway, Birmingham B4 6NN, UK [e] School of Dentistry and Stomatology, Université catholique de Louvain, Brussels, Belgium * corresponding author. Contact: luc.randolph@uclouvain.be

Highlights:

- Filler characteristics greatly vary amongst the 17 resin composites analyzed
- Mechanical properties varied by up to a factor 3 amongst materials
- Materials differed in their sensibility to incubation medium (water or EtOH/water)
- The filler content ($W_{fillers}$) was confirmed as major discriminatory characteristic
- A simple classification and terminology can be suggested based solely on $W_{fillers}$

Abstract: Objectives

The mechanical properties of dental resin-based composites (RBCs) are highly dependent on filler characteristics (size, content, geometry, composition). Most current commercial materials are marketed as "nanohybrids" (i.e. filler size < 1μm). In the present study, filler characteristics of a selection of RBCs were described, aiming at identifying correlations with physico-mechanical properties and testing the relevance of the current classification.

Methods

Micron/sub-micron particles (> or <500nm) were isolated from 17 commercial RBCs and analyzed by laser diffractrometry and/or electron microscopy. Filler and silane content were evaluated by thermogravimetric analysis and a sedimentation technique. The flexural modulus (E_flex) and strength (σ_flex) and micro-hardness were determined by three-point bending or with a Vickers indenter, respectively. Sorption was also determined. All experiments were carried out after one week of incubation in water or 75/25 ethanol/water.

Results

Average size for micron-sized fillers was almost always higher than 1μm. Ranges for mechanical properties were: 3.7<E_flex^water<16.3GPa, 86<σ_flex^water<161MPa and 23.7<〖hardness〗^water<108.3HV0.2/30. Values generally decreased after storage in ethanol/water (Δ_max = 86%). High inorganic filler contents (>75wt%) were associated with the highest mechanical properties (E_flex and σ_flex > 12GPa and 130MPa, respectively) and lowest solvent sorption (~ 0.3%).

Significance

Mechanical properties and filler characteristics significantly vary amongst modern RBCs and the current classification does not accurately illustrate either. Further, the chemical stability of RBCs differed, highlighting differences in resin and silane composition. Since E_flex and sorption were well correlated to the filler content, a simple and unambiguous classification based on such characteristic is suggested, with three levels (ultra-low fill, low-fill and compact resin composites).

Keywords: resin-based composite; composite; nanohybrid; classification; filler characteristics; nano particles; fillers; size distribution; size; mechanical properties; flexural modulus; flexural strength; degradation; sorption

I. Introduction

The popularity of dental resin composites is driven by their versatility, aesthetic quality and reasonable clinical performance. The development of resin composite materials are relentlessly researched and tested by academia and industry in an attempt to enhance clinical longevity by reducing their perceived shortcomings such as polymerization stress [1, 2], residual monomer content [3, 4], inadequate depth of cure [5], handling [6] and aesthetic characteristics [7]. Most often, these issues are not entirely addressed and new concepts aggressively marketed as “low-shrink” or “bulk-fill” and such. The resin composite market is highly competitive between manufacturers, and the incredibly rapid and iterative product cycle leaves the general practitioner with a vast choice from an array of similar materials types. As a consequence, and particularly for resin composites, the usefulness of classification systems as a means for practitioners to compare material properties is limited.

An area of substantial development since the inception of resin composite materials relates to filler type, processing and morphology, and probably much more so than advancements in resin chemistry. Continuous material developments among researchers and manufacturers have led to the use of refined filler technologies and design choices. Following the evolution of processing techniques, the size of filler particles, typically ground glasses, have decreased from tens of micron to about 1 μm [8]. With advancements such as jet-milling, sub-micron dimensions can be achieved with narrow distributions and microparticles averaging 0.5-1.0 μm are now used in some commercial composites. Pre-polymerized fillers (PPF) are also common and processed using ground cured composite, containing a variety of sub-micron particles. Such particles were introduced in part as a solution to reduce the stress resulting from polymerization and provide improved polishability compared with earlier hybrid types [9, 10]. Nanoparticles, originally introduced in an effort to improve aesthetic quality are used today in some modern materials in the form of nano-sized aggregates, aimed at improving mechanical properties, in particular strength [11]. Discrete nano-sized fillers, smaller than the wavelength of visible light, represent an additional asset in light-curing materials, since refraction and scattering are reduced, which may offer significantly improved depth of cure [12].

The classification of dental composite has evolved over the years, but in general has mostly focused on filler-size distribution, filler content or composition. From "microfills" or "nanofills", containing only micro or nanoparticles, respectively, most modern resin composites belong to a so-called "hydrid" category, and presently are commonly marketed as "nanohybrids". This terminology refers to materials containing a fraction of nanoparticles (< 100 nm) and of sub-micron particles (≤ 1 μm, typically averaging 0.5-1.0 μm) [8] (Figure 1). Compared to "microhybrids", nanohybrids can be expected to contain a greater fraction of nanoparticles. However, a classification based on filler-size distribution does not reflect filler composition, morphology or filler specificities (eg the use of PPF). It is therefore doubtful for

example that all nanohybrids would display the same properties and many commercial resin-based composites (RBCs) claiming to be "nanohybrids" will have a significant proportion of larger size (> 1 µm) fillers [13, 14].

There is in fact a vast bank of data documenting various mechanical and physical property comparisons. These properties vary greatly from one material, or test-center, to another. For example, the flexural modulus measured in-vitro ranging from 3 to 15 GPa [15-17] or flexural strength, hardness or fracture toughness also varying, between 50 to 150 MPa [13, 15, 17, 18], 19 to 80 HV0.5/20 [17] and 1 to 2.5 MPa.$\sqrt{m}$ [17, 18] respectively. These properties are interrelated and dependent on filler characteristics (geometry, composition, surface coating, size distribution) and filler content (filler mass and volume content). Excellent studies have covered the topic and general rules are that both the modulus and surface hardness increase with increasing filler content with a concomitant decrease in volumetric shrinkage [17, 19]. At a given filler content, size and geometry, strength is influenced by the chemistry of the resin phase [20-22]. A biomimetic approach would advocate similar properties of resin composites such as rigidity and strength compared with the tissue they replace, i.e. mostly dentin, for which the modulus and strength were placed in the range of 20-25 GPa (Young's modulus) and 52-105 MPa (ultimate tensile strength) [23]. Most difficult to achieve and embodying the major challenge of composites, such high moduli RBCs would also need to display similar toughness than dentin (1.5-2.7 MPa.$\sqrt{m}$ [24]) at the risk of otherwise being too brittle. Also of some importance, the mechanical properties of composites should not degrade with time and should be chemically stable. In-vitro studies have repeatedly demonstrated that depending on materials characteristics, the response of RBCs to mechanical and chemical challenges vary. Recent work has highlighted the degradation of strength of commercial materials following fatigue tests to well below the 80 MPa limit set by ISO 4049 [18]. In addition, great variations in the strength measured were observed between materials. Regarding chemical stability, solvent sorption has

been extensively investigated as a tool to determine a material's hydrophobicity. It has been suggested that solvent sorption is directly correlated to the extent of hydrolytic effects, altering mechanical properties [25]. Characterizing a composite's solvent uptake could therefore provide a tool to infer mechanical performance.

Some studies have investigated the mechanical properties of a panel of commercial resin composites in relation to filler content and morphology [13, 15, 26, 27], however none have recently characterized filler distribution or related mechanical properties correlations. Consequently, the aim of the present study was to characterize the physical and mechanical properties of a wide selection of modern, "nanohybrid" dental composites in relation to filler content, filler morphology and distribution. A subsequent aim was to propose a new classification based on the correlations between these various characteristics.

II. Materials and Methods

This work intended to include a list of "nanohybrids" composite materials as diverse in composition as possible. 17 different resin composites were selected for the present study (Table 1).

1) Determination of filler content

The determination of inorganic content was carried out using two complementary methods, firstly, thermogravimetric analysis [15]. Small amounts of material (typically 50-100 mg) were placed in a temperature-controlled chamber. The weight of material was monitored as temperature increased to 900 °C. Inorganic content (W_i, in wt%) was determined as the remaining weight of matter relative to the initial amount (n = 3). A transition located around 400 °C (typically between 380-480 °C) was also quantified and tentatively associated with the

degradation of silanes (transition verified with Aerosil R 7200, Figure 2, also in line with other results [28, 29]).

Given the limitations in filler processing techniques, it was assumed there would be a sharp step in filler distribution at about 500 nm, it being the lower bound in the range of sub-micron ground particles. Particles were separated around that threshold: fillers were extracted and their respective amounts determined by dissolving the resin composites in acetone and separating each filler type by gravimetry (>500 or <500 for particles with a size greater or smaller than 500 nm, respectively). Briefly, for one measurement, 0.3 g of resin composite was placed in 10 mL acetone (precision 0.0001 g). The tube was vortexed until all the material was fully dispersed. Two centrifugation cycles were employed, first to obtain the >500 fillers (3000 g for 1 min) followed by another (5000 g for 30 min) to collect <500 fillers. One should note that due to the limitation in centrifugation speed, some of the smallest non-aggregated nanoparticles may not have been collected. To completely remove any soluble content, once separated, the fillers were washed twice with acetone and re-centrifuged at high speed. Powders were recovered by allowing the suspensions to dry under a fume hood at room temperature for 24 h. Total weight filler content (W_{total}) was then determined, corresponding to the sum of >500 and <500 fillers ($W_{>500}$ or $W_{<500}$ respectively).

2) Filler size distribution and morphology

The separated fillers were characterized by laser diffraction and scanning electron microscopy (SEM). The first method informed on the size distribution of the >500 fillers and the second on the geometry of both filler types. For laser diffraction, >500 fillers were re-dispersed in ethanol, sonicated to maximize particle de-aggregation and analyzed using a particle size analyzer (0.25-85 µm range, HELOS, Sympatec GmbH). The installed software (Windox 5, Sympatec GmbH) provided cumulative volume distributions ($Q(x)$), with x the

particle size). To obtain distribution densities ($q(x)$), which graphically are easier to interpret. Equation 1 was used:

$$(1)\ q(x) = \frac{dQ(x)}{dx}$$

To transform the abscissa in a logarithmic scale. Equation 2 was applied:

$$(2)\ q(\ln(x_{i-1}), \ln(x_i)) = \frac{Q(x_i) - Q(x_{i-1})}{\ln\left(\frac{x_i}{x_{i-1}}\right)}$$

The distribution densities where normalized, dividing values by the maxima. If one peak was observed for a distribution, it was described as "monomodal". If two peaks could be distinguished from a distribution density, then it was considred that two different size regimes existed and the distribution was described as "bimodal". Additional distribution characteristics were also provided by the software. Three are presently reported, denoted as d_α (in µm), which describe the diameter where α vol% of the distribution has a smaller particle size.

SEM analysis on the separated particles was carried out by dropping small amounts of powders on carbon tape, which were then carbon coated. The accelerating voltage varied between 5 to 15 kV (JEOL 7600F, JEOL, Japan), depending on the contrast needed.

3) Mechanical properties

All resin composites were photo-polymerized using a LED light-curing unit (Bluephase G2, Ivoclar Vivadent, Liechtenstein). Irradiance and exposure time were 1000 ± 50 mW/cm^2 and 20 seconds, respectively. The irradiance was controlled using a thermal power sensor (S310 C, Thorlabs) and the evolution of irradiance as a function of time can be observed in Figure S1.

The flexural modulus and flexural strength were determined using a universal testing machine (LRX Plus, Lloyd Instrument) equipped with a three-point bending jig. Twenty specimens per material of dimensions 25 mm length, 2 mm width, 2 mm thickness were

prepared in white Teflon split-moulds by photo-polymerizing using three non-overlapping irradiation cycles (tip diameter = 10 mm). Cured specimens were polished using SiC paper grit 1000. Prior to testing, half of the specimens were incubated in distilled water and the other half in 75/25 vol% ethanol/distilled water, both for 1 week at 37°C (n = 10). The specimens were loaded on a 20 mm support-span (knife edge geometry) at a 0.75 mm/min cross-head speed. Flexural modulus (E) and flexural strength using Equation 3 and 4:

$$(3)\ E_{flex}^{i}\ (GPa) = \frac{L^3 * \delta}{4 * w * t^3 * 1000}$$

with *L*, *w* and *h* the distance between supports, *w* and *t* the width and thickness of the bars (all in mm). δ was the slope of a force/deformation curve in the elastic region (N/mm). i denotes the incubation medium used. The flexural strength was calculated using Equation 4:

$$(4)\ \sigma_{flex}^{i}\ (\mathrm{MPa}) = \frac{3 * F_{max} * L}{2 * w * t^2}$$

with F_{max} (N) the maximum force sustained before failure was observed.

Surface hardness was determined using a Vickers indenter (Durimet, Leitz, Wetzlar, Germany). Cylindrical specimens (2 mm thick, 5 mm in diameter) were photo-polymerized in one cycle. Cured and unpolished specimens were incubated identically to the bars (n = 3). Following incubation in the different mediums, the disks were indented for 30 s using a 200 g load. For each specimen a hardness value was determined using Equation 5:

$$(5)\ HV\ (0.2/30) = \frac{0.1854 * 0.2}{d^2}$$

where d is the averaged diagonal of three indentations in mm.

4) Solvent uptake

Water and ethanol/water sorption was evaluated in order to indirectly determine the hydrophobicity of materials associated with the amount and nature of the organic fraction

(matrix and silanes). Similarly to Sideridou et al. [28], samples (identical to the disks prepared for the hardness measurements) were light-cured, weighed (m_1, precision 0.0001 mg) and immediately placed in distilled water or a 75/25 vol% ethanol/distilled water solution in the wells of a 48-wells plate (1 mL/disk/well, n = 3). After one week at 37 ± 1 °C, materials were removed from the solvents, blotted dry and re-weighed (to determine m_2) and then left to dry over silica gel in a vacuum chamber. Disks were regularly weighed and when values stabilized, final weights were determined (m_3). The determination of solvent sorption (S) and released matter (R) was carried out using Equation 6 and 7:

(6) $S\ (\%) = \frac{m_2 - m_3}{m_1}$

(7) $R\ (\%) = \frac{m_1 - m_3}{m_1}$

Due to adsorbed solvent that could not be removed even after several weeks under vacuum, $m_3$values could remain higher than related m_1. This flawed the calculation of S and R and associated data were therefore not reported.

5) Statistical analysis

The datasets were checked for normality using the Shapiro-Wilk test. Means were compared using Tukey's test and selecting 0.05 as significance level. The JMP 11 software (SAS Inc.) was used for all statistical analyses.

III. Results

1) Filler content

The determination of inorganic content by TGA showed large differences, with values varying between 52.2 wt% and 88.1 wt%, with an average $\overline{W_{total}}$ = 73.5 wt% (Table 2). While two of the "flowable" materials (*ELS Flow* and *Diamond Flow*) were found among those

containing the smallest inorganic content, consistent with their apparent low viscosity, two others were highly filled (≥ 75 wt%, *Grandio Flow* and *Exp. Flow LC*). Inversely, materials found as rather viscous pastes were associated with low inorganic contents (for example *Gaenial* with 57.8 wt %). Three materials presented major discrepancies between their W_i and W_{total}, between 16 wt% for *Gaenial*, and ~ 10 wt% for *Kalore* and *Tetric Evo Ceram* (Table 2). The determination of $W_{>500}$ and $W_{<500}$ by sedimentation also showed large variations in composition. Generally, $W_{>500}$ accounted for most of W_{total}, in particular for the *Venus Diamond Flow*, for which $W_{<500}$ was close to zero (Table 2). On the contrary, the *Clearfil Majesty Flow* was found to contain a majority of sub-micron particles ($W_{<500}$ = 41.4 wt% and $W_{total} \sim W_i \sim$ 67 wt%). In comparison, for the remainder of the materials, the fraction of <500 particles was lower than 20 wt%.

2) Filler morphology and size distribution

SEM analysis revealed different morphologies for the micro and nano fillers (Figure 3), which varied between spherical to rough and irregular particles. Except for the material with spherical micro fillers (*Clearfil Majesty Flow*), the irregular particles displayed a range of sharpness in their geometry (Figure 3a). Regarding particle dimensions, the largest particles observed were in the range of the tens of microns in several materials. In the others, the largest did not exceed 1 µm (*ELS Flow* for example).

SEM analysis also revealed pre-polymerized fillers within the materials for which $W_i << W_{total}$ and the *Venus Pearl* (Figure 3b). Sub-micron particles were identified within the PPFs of *Kalore* and *Tetric Evo Ceram*. In the *Gaenial* and *Venus Pearl*, the PPF surface appeared smoother than in the two other composites and very fine particles could be observed (~100 nm). Three "types" of nano fillers could be clearly identified (Figure 3c): true nanoparticles (< 100 nm), aggregates or "nanoclusters" and what appeared as ultra-fine ground particles (100-400

nm). For the "true" nanoparticles, aggregation was observed. The diffuse boundaries were attributed to the preparation method (solvent evaporation and metallic coating).

Significant differences in term of particle size and size distribution for the micro particles (> 500 nm) could be observed from the analysis of the separated fillers by laser diffractometry (Figure 4). The distribution density plotted as a function of particle size showed that all materials presented at least one peak centered at about 1-2 µm. In some cases minor peaks were observed around 10 µm and were associated with aggregates remaining after sonication (Figure 6a). Further, a second peak located at higher dimensions was observed in several materials (Figure 6b), corresponding to larger micro fillers. Their mean average size varied between 5 µm and 30 µm. The distribution characteristic d_{90} (in µm) indicated similar groups: the *Admira Fusion*, *ELS*, *ELS Flow*, *Exp. Flow LC*, *Exp. LC* and *Venus Diamond Flow* had 90 vol% of their fillers smaller than 5.0 µm (Table 3). Due to particle aggregation, the *Filtek Silorane* and *Venus Pearl* had a d_{90} of 6.0 and 8.7 µm, respectively. The *Clearfil Majesty Posterior* and *Filtek Supreme XTE* both presented a d_{90} value of 7.2 µm. Finally, the *Clearfil Majesty ES Flow*, *Gaenial*, *Grandio*, *Grandio Flow*, *Kalore*, *Tetric Evo Ceram* and *Venus Diamond* had d_{90} values greater than 10 µm.

3) Mechanical properties

The mechanical properties varied greatly from one material to another. Determined under flexure after an aqueous incubation, E_{flex} varied between 3.7 GPa (*ELS Flow*) and 16.3 GPa (*Grandio*, *Clearfil Majesty*). σ_θ varied between 87 MPa (*Grandio Flow*) and 168 MPa (*Venus Diamond*) (Table 4). The Vickers hardness varied between 23.7 HV 0.2/30 (*Venus Diamond Flow*) to 108.3 HV 0.2/30 (*Clearfil Majesty*). When using a 75/25 ethanol/water incubation medium, the mechanical properties generally decreased. Ranges for E_{flex} and σ_θ became 0.7-15.0 GPa and 13-139 MPa, respectively. The highest drop between incubation medium for E_{flex}

and σ_θ were 82 and 88 % (Table 5). For hardness, values fell between 8.0-106.7 HV 0.2/30 with a highest drop of 65 %.

4) Solvent uptake

Water sorption varied between 0.25 % (*Clearfil Majesty*) and 0.99 % (*Gaenial*), while ethanol/water sorption varied between 0.35 % (*Clearfil Majesty*) and 2.31 % (*ELS Flow*) (Table 6). For the *Grandio* and *Filtek Supreme XTE*, water or ethanol/water sorption was similar. The release of soluble matter in water varied between 0.02 % (*Clearfil Majesty*) and 0.28 % (*Grandio Flow*), while higher values were measured overall in ethanol/water, varying between 0.14 % (*Grandio)* and 0.89 % (*ELS*).

IV. Discussion

The analysis of fillers isolated from the resin composites was carried out with two objectives, first to investigate potential correlations between filler characteristics and physico-mechanical properties, also in relation to the incubation medium. The second objective was to check the suitability of filler characteristics as basis for material classification.

1) Filler characteristics & mechanical properties

In the present study, the characterization of 17 materials marketed as "nanohybrids" showed that the fillers used were vastly different with regards to their shape (Figure 3), content, distribution and ratio of micro and nano-sized particles (Tables 2 and 3). Still, in order to investigate potential correlations, it would be most helpful to identify groups of materials based on one or more filler characteristics. The current classification for resin composites currently relies on filler size to generate classes of material. As described earlier, the micro- and nanohybrid discrimination refers to the size of the largest micron-sized particles, limited to 1 µm for the nanohybrids. Presently, two categories of materials were observed, relating to this classification: one group with a size limited to 1-2 µm (Figure 4a) and another with much larger

particles, up to 30 µm (Figure 4b). These materials will be referred to as displaying "monomodal" and "bimodal" distributions, strictly in reference to the micro particles. Other characteristics such as filler content or filler morphology varied without any obvious trend. For example, while manufacturers made efforts to maximize filler content, it nevertheless overall varied between 52.2 wt% and 88.1 wt%. Hence, it would instead be very convenient for translational purposes (for practitioners) if the physico-mechanical properties of the resin composites could be predicted based on filler size distribution. However, as will be discussed below, this may not be a relevant approach based on the present results.

The modulus of resin composites designed for load bearing restorations should be as close to that of the tooth (20-25 GPa [23]), to encourage a homogeneous stress-distribution at the tooth-restoration interface [30]. In composites, mechanical properties are determined based on the intrinsic properties of the different phases and their volume fractions. This "Rule of mixtures" applied to composites for example stipulates that the modulus increases with filler content, according to:

(8) $E_{composite} = V_{fillers}E_{fillers} + \left(1 - V_{fillers}\right)E_{resin}$

with $V_{fillers}$ the volume fraction of fillers and considering ideal stress distribution between the resin and filler phases. However, once the largest particles are in contact and the packing fraction has reached the theoretical 0.74 vol% limit, the modulus of the composite would increase non-linearly, rapidly getting closer to that of the fillers [31]. This trend can be clearly observed in Figure 5a, whilst noting the abscissa displays mass contents. Values for the "unimodal" and "bimodal" distributions appeared scattered, without a definite separation between the two groups, contradicting the classification. Interestingly, the materials containing PPF displayed relatively low flexural moduli given their high filler contents (W_{total}) and densities (Table 2). This is of course associated to the lower modulus of the PPF compared to

glass particles. Whether PPF particles should be considered as fillers remains debatable and will be discussed in Section 2 of the discussion.

When considering σ_{flex}^{water}, no general trend could be observed between the strength and filler content (Figure 5b) or size distribution. The lack of general trend could be attributed to the differences in W_i at similar size distribution, difference in matrix composition but also the sensitivity of strength measurement in relation to specimen surface preparation. In three materials however, a relatively high modulus and strength could be observed ($E_{flex}^{water} \geq 10$ GPa; $\sigma_{flex}^{water} \geq 130$ MPa, observed for the *Venus Diamond*, the *Grandio* and *Clearfil Majesty Posterior*), which were associated with high densities (2.1-2.4 g/cm^3) and W_i (73-88 wt%), but also relatively low d_{90} values (Table 3 and Figure 4). While it would be adventurous to definitely associate these results to specific size distributions given the variations in W_i (all three materials have bimodal distributions), the likeliness of the three characteristics to fall in similar ranges coincidentally for these materials is quite low. Since an increase in filler content requires the optimization of size distribution, a decrease in filler size and adapting the filler/resin interface, the case of the three noted materials highlight the influence of these characteristics on strength. Finally, micro hardness testing evaluates the resistance to plastic deformation under a given load. Consequently, this property should be strongly correlated to the filler content, accepted that fillers are of the same dimension than the indentation. This was presently not clearly observed (Figure 5c). However, although no influence from micro particle size distribution could be determined, a strong correlation (0.89, spearman correlation coefficient) was observed between E_{flex}^{water} and $hardness^{water}$, which underlined the existence of one or more common factors (0.86 in ethanol/water). This falls in line with results from another study [17] and the trend between the elastic modulus and W_i was shown above. Amongst the possible reasons for the lack of correlation between filler content and the hardness, differences in the composition of glasses used between materials is one of the possible explanations. This once again confirms

the difficulty of comparing the impact of one single variable (e.g. W_i) on a given property among a population of commercial materials, where so many variables (filler shape and composition, photoinitiation system, monomer type and ratios, etc) differ at the same time [32].

Ideally, resin composites must be chemically stable and their mechanical properties should not exhibit significant deterioration after aging. Many previous works have studied the impact of aqueous immersion on mechanical properties [33-35]. While a hydrolytic effect has been postulated, there is little data to support it: a thorough recent study investigating monomer elution failed to observe any breakdown products, even after 180 days of incubation [4]. However, the use of an ethanol or organic-based solution has previously been associated with major degradation in mechanical properties [34, 36]. Researchers have postulated either silane or matrix degradation, and therefore a combination of incubation mediums was chosen in the present study to check for chemical stability. Regarding duration, it is known that resin composites continue to polymerize for 24 h following irradiation [37, 38] but sorption occurs over a longer time scale [39]. In the present study we selected a 1-week incubation period following previous works [3, 40], with the specimens being rapidly immersed to mimic clinical settings as post-curing occurs while saliva is in contact with the restoration. Chemical aging may affect the structural integrity of the organic phase, and when tested, a sample would fail due to an overall degraded matrix and/or interface. When plotting losses for mechanical properties between the water and organic incubation as a function of silane content or inorganic content (Figure 6), a general trend of increasing losses with increasing contents could be observed. This was more obvious with the organic content, although no significant trend could be determined. Similarly to the differences amongst glasses used for the fillers, the type of silane and thickness of the deposited layer is highly likely to vary amongst resin composites. For these reasons, determining an overall correlation among commercial materials would be difficult. In addition, due to the tentative nature of the quantification, values for the silane

contents may deviate from those actually used. For example, low molecular weight monomers may degrade at the same temperature as silanes. Some further work could focus on determining the type silanes and surface coverage of fillers, for example by using spectroscopy methods. This is however beyond the scope of the present study and another property, namely solvent sorption was used to provide some further information on the resin composites.

Solvent sorption was investigated in order to indirectly shed some light on the composition and stability of the organic fraction of the resin composites. The types of monomers and silanes used greatly influence how much the cured networks will absorb and swell [25] and the greatest sorption will occur when the solubility parameter between the solvent and the constituents of a resin composite is greatest. By analyzing water and ethanol-water sorption along with its relation to flexural strength, one could infer the extent of sorption, swelling and network breakdown effects. Among the materials studied, a definite increase in solvent sorption with increasing organic content could be observed (Figure 7a), again with no obvious influence from the filler size distribution. At similar organic contents, small differences in water sorption were seen. Larger differences were however noted for the ethanol-water sorption (the slope of the linear fit was 2 times higher). In both solvents these differences would be associated to variations in network characteristics such as cross-link density, distance between cross-links and overall conversion of both the filler-bound and free reactive groups [25, 41]. The increased solubility with the ethanol-water mixture ($R_{ethanol/water} >> R_{water}$, Table 6) likely exacerbated the compositional differences between materials due to greater swelling. Further, when plotting σ_{flex} of the resin composites as a function of solvent sorption (Figure 8b), an overall decrease with increasing solvent uptake could be observed. With these results, while it remains difficult to conclude on any specific additional breakdown effects in the presence of ethanol, impacting σ_{flex}, it could however be hypothesized that the more the resin matrices and filler-resin interface swelled, the weaker they were. Statistical analysis indicated negative

correlations between sorption and σ_{flex} (-0.54 and -0.79 for water and ethanol-water incubation mediums, Spearman correlation coefficient, $p<0.0001$ in both cases). Interestingly, when plotting the σ_{flex} losses as a function of the ratio ethanol-water to water sorption, a general increasing trend could be observed (Figure 7c). Stated differently, materials for which the lowest losses were observed also displayed similar solvent intakes in both media (ratio ~ 1). In addition, these materials (*Grandio* and *Filtek Supreme XTE*) also absorbed less solvent and were amongst the most heavily filled. Hence, this evidence again supports the maximization of filler content and highlights that some materials contain monomers and silanes that are more stable in both water and ethanol. The differences in mechanical properties and resistance to degradation may also be attributed to other structures than the polymer network. For example, the presence of stress-absorbing structures may also affect strength and crack propagation. It has for example been reported that the *Filtek Supreme XTE* contains nanoclusters made of agglomerated nanoparticles (Figure 3c) [42]. Such structures, whether they may be chemically or physically aggregated, can impede crack propagation by absorbing stress through fragment splitting from the main cluster and crack bifurcation [11]. Finally, the release of matter from the cured resin composites was only poorly correlated to organic content or sorption, for both the water and ethanol/water incubation. As the extent of photopolymerization defines the amount of remaining free monomers, the lack of correlation would in part indicate a varying extent of conversion between materials. Beside conversion differences among materials, variations such as monomer type and ratio would here also greatly influence the release of un-reacted species.

2) Resin composite classification

In the first part of this study, it was repeatedly shown that amongst materials marketed as "nanohybrids", there were major differences in mechanical properties and stability in solvents.

The final part of this work will discuss whether any of the material characteristics investigated earlier may be suitable as basis for a new classification.

For the various existing resin-composite classifications, filler size seems to be the most frequently used criteria [8]. However, the present results have shown that it neither relates to mechanical properties nor water or ethanol-water sorption. Further, such classification is not even strictly followed, with some manufacturers mislabeling their materials as "nanohybrids", instead of the more appropriate "microhybrids" terminology due to the presence of particles much larger than 1 µm (Figures 3 and 4). Based on the present results, the inorganic filler content appears as a more appropriate predictor than filler size, with a clear correlation with both E_{flex} and sorption. Such as classification (irrespectively of filler type and size), would also indirectly give some qualitative information about the quality of the filler technology used, since maximizing filler content while maintaining clinically relevant rheological properties requires progress in size distribution as well as in the quality and chemistry of the resin-filler interface. For some manufacturers however, aesthetics, handling or other properties are regarded as central features, leading to varying material design choices. Most notably, PPF were introduced to improve polishability [43], gloss and potentially limit the development of polymerization stress [44]. Another potential role of PPF would be to increase light scattering, and thereby improve the optical transition with the tooth. However composites used to prepare PPF are cured and ground well before a PPF-containing composite is actually photopolymerized in the oral cavity. This means that PPF lack active binding sites, are difficult to silanize, which in turn equivocates to a poor integration in the resin matrix. As it was observed in the present study and elsewhere [45], most PPF-containing materials display relatively low E_{flex} and σ_{flex} considering their apparent filler content (w_{total}). It follows that in a classification based on the filler content as discriminative characteristic, only the particles with an elastic modulus well above that of the organic phase could be considered as reinforcing fillers. The introduction of

other compounds beside PPF, for example inorganic-organic monomers (condensed methacryl silanes [46]) also represents a challenge for classification (for example the "Ormocer" *Admira Fusion*). Other molecules such as polyhedral oligomeric silsesquioxane (POSS) could lead to similar classification issues. Hence, for such classification to be efficient to predict material properties, it becomes necessary to associate filler content to a specific property, evidently advocated here to be the elastic modulus. In other words, for a compound to be considered as reinforcing filler, its introduction should improve the elastic modulus compared to the same material without it. Whether or not this filler content/elastic modulus combination is most suitable can be discussed, since other properties such as fatigue resistance or fracture toughness are crucial properties. In any case we support for a similar rationale to be considered and observed when conceiving any classification.

Finally, defining the terminology of the classification for dental resin composites is also of some importance. Ideally, the terminology used should also participate to inform the reader or consumer on the important material properties. The term "hybrid", currently under use, is rather unclear and the use of "nano" is delicate given the disagreements regarding its use in dentistry. The aim presently is not to discuss at depth semantics: given the basis advocated above, namely the use of filler content as an indicator of material properties, one needs a scale against which to grade a material. For the filling of a material and if particle dispersion was to be optimal, there is a theoretical threshold of 74 vol%, a packing limit. A second and arbitrary level could be set at 50 vol%, as the balance between φ_{resin} and φ_{filler}. Below this limit, a material may be termed "ultra-low fill" (Figure 8). At $50\ vol\% < \varphi_{resin} < 74\ vol\%$, a material could be referred to as "low-fill". At 74 vol%, the material may be termed "compact". In practice, since perfectly homogeneous resin composites cannot be obtained, one should keep in mind that increases in filler content will necessarily be obtained by using different size regimes, all materials being therefore "hybrids" in any case. Higher values than 74 vol% could hence be

obtained (such as with the *Clearfil Majesty Posterior*, Table 1 bis). Further, reaching high filling contents requires the best efforts in silanization. A "compact" composite would likely also present low sorption values and possibly greater stability and durability under chemical challenges.

Additional terms could potentially be added to fine-tune a description. Such terms may inform on other important clinical aspects such as rheological characteristics ("fluid", "packable", "flowable", etc) or polishability. A material such as the *Grandio Flow* could for example be labeled as a "compact flowable".

Conclusion

The characterization of filler particles characteristics showed that over a wide range of tested commercial resin composites, particle size, shape, distributions and contents greatly vary. The E_{flex} and σ_{flex} were measured in the range 3.7-16.3 GPa and 86-161 MPa, respectively after storage in water. Lower values were observed after storage in 75/25 vol% ethanol/water, but not for all materials. The resin composite with the highest properties also had the highest filler contents and exhibited the lowest solvent sorption. Currently, the most used classification is based on particle size distribution. Mechanical properties were however not correlated to it. Instead, the filler content appeared better suited as basis for classification, it being correlated to the flexural modulus and solvent sorption. Sorption was also linked to the flexural strength, with increasing sorption levels being associated to decreasing strength, highlighting the importance on limiting solvent uptake.

Based on these results, a simple and unambiguous classification was suggested, based on the filler content and using two levels: 50 and 74 vol%. The terms *ultra-low fill*, *low-fill* and *compact* resin composites would apply to materials with filler contents lower or higher than 50 vol% or higher than 74 vol%, respectively. With this classification, or one similar, the terminology is more likely related to a material's physico-mechanical properties. Finally, the

various functional agents introduced in modern dental composites need to be characterized for their effect on the said properties. For example, particles introduced to improve polishability on the one side, but which impact mechanical properties on the other side cannot also be considered as reinforcing fillers.

Acknowledgments

L.D. Randolph is a FRIA (F.R.S-FNRS) scholar. The authors would like to thank the manufacturers for supplying the resin composites. This study was partially supported by GC, Heraeus-Kulzer, Saremco dental and VOCO GmbH.

References

1. Goncalves, F., C.C. Pfeifer, J.W. Stansbury, S.M. Newman and R.R. Braga, *Influence of matrix composition on polymerization stress development of experimental composites.* Dent Mater. 26 (2010) 697-703.
2. Eick, J.D., S.P. Kotha, C.C. Chappelow, K.V. Kilway, G.J. Giese, A.G. Glaros and C.S. Pinzino, *Properties of silorane-based dental resins and composites containing a stress-reducing monomer.* Dent Mater. 23 (2007) 1011-1017.
3. Randolph, L.D., W.M. Palin, S. Bebelman, J. Devaux, B. Gallez, G. Leloup and J.G. Leprince, *Ultra-fast light-curing resin composite with increased conversion and reduced monomer elution.* Dent Mater. 30 (2014) 594-604.
4. Sevkusic, M., L. Schuster, L. Rothmund, K. Dettinger, M. Maier, R. Hickel, K.L. Van Landhuyt, J. Durner, C. Hogg and F.X. Reichl, *The elution and breakdown behavior of constituents from various light-cured composites.* Dent Mater. 30 (2014) 619-31.
5. Leprince, J.G., P. Leveque, B. Nysten, B. Gallez, J. Devaux and G. Leloup, *New insight into the "depth of cure" of dimethacrylate-based dental composites.* Dent Mater. 28 (2012) 512-520.
6. Lee, J.-H., C.-M. Um and I.-b. Lee, *Rheological properties of resin composites according to variations in monomer and filler composition.* Dent Mater. 22 (2006) 515-526.
7. Mikhail, S.S., S.R. Schricker, S.S. Azer, W.A. Brantley and W.M. Johnston, *Optical characteristics of contemporary dental composite resin materials.* Journal of Dentistry. 41 (2013) 771-778.
8. Ferracane, J.L., *Resin composite--state of the art.* Dent Mater. 27 (2011) 29-38.
9. Senawongse, P. and P. Pongprueksa, *Surface roughness of nanofill and nanohybrid resin composites after polishing and brushing.* J Esthet Restor Dent. 19 (2007) 265-73; discussion 274-5.
10. Ferracane, J.L., C.S. Pfeifer and T.J. Hilton, *Microstructural Features of Current Resin Composite Materials.* Current Oral Health Reports. 1 (2014) 205-212.

11. Curtis, A.R., W.M. Palin, G.J. Fleming, A.C. Shortall and P.M. Marquis, *The mechanical properties of nanofilled resin-based composites: the impact of dry and wet cyclic pre-loading on bi-axial flexure strength.* Dent Mater. 25 (2009) 188-97.
12. Fujita, K., T. Ikemi and N. Nishiyama, *Effects of particle size of silica filler on polymerization conversion in a light-curing resin composite.* Dent Mater. 27 (2011) 1079-85.
13. Kim, K.H., J.L. Ong and O. Okuno, *The effect of filler loading and morphology on the mechanical properties of contemporary composites.* J Prosthet Dent. 87 (2002) 642-9.
14. Scougall-Vilchis, R.J., Y. Hotta, M. Hotta, T. Idono and K. Yamamoto, *Examination of composite resins with electron microscopy, microhardness tester and energy dispersive X-ray microanalyzer.* Dent Mater J. 28 (2009) 102-12.
15. Leprince, J., W.M. Palin, T. Mullier, J. Devaux, J. Vreven and G. Leloup, *Investigating filler morphology and mechanical properties of new low-shrinkage resin composite types.* J Oral Rehabil. 37 (2010) 364-76.
16. Ilie, N., A. Rencz and R. Hickel, *Investigations towards nano-hybrid resin-based composites.* Clin Oral Investig. 17 (2013) 185-93.
17. Jun, S.-K., D.-A. Kim, H.-J. Goo and H.-H. Lee, *Investigation of the correlation between the different mechanical properties of resin composites.* Dental Materials Journal. 32 (2013) 48-57.
18. Belli, R., A. Petschelt and U. Lohbauer, *Are linear elastic material properties relevant predictors of the cyclic fatigue resistance of dental resin composites?* Dent Mater. 30 (2014) 381-91.
19. Shah, P.K. and J.W. Stansbury, *Role of filler and functional group conversion in the evolution of properties in polymeric dental restoratives.* Dent Mater. 30 (2014) 586-93.
20. Pfeifer, C.S., L.R. Silva, Y. Kawano and R.R. Braga, *Bis-GMA co-polymerizations: influence on conversion, flexural properties, fracture toughness and susceptibility to ethanol degradation of experimental composites.* Dent Mater. 25 (2009) 1136-41.
21. Ruttermann, S., I. Dluzhevskaya, C. Grosssteinbeck, W.H. Raab and R. Janda, *Impact of replacing Bis-GMA and TEGDMA by other commercially available monomers on the properties of resin-based composites.* Dent Mater. 26 (2010) 353-9.
22. Asmussen, E. and A. Peutzfeldt, *Influence of UEDMA BisGMA and TEGDMA on selected mechanical properties of experimental resin composites.* Dent Mater. 14 (1998) 51-6.
23. Kinney, J.H., S.J. Marshall and G.W. Marshall, *The mechanical properties of human dentin: a critical review and re-evaluation of the dental literature.* Crit Rev Oral Biol Med. 14 (2003) 13-29.
24. Nalla, R.K., J.H. Kinney and R.O. Ritchie, *Effect of orientation on the in vitro fracture toughness of dentin: the role of toughening mechanisms.* Biomaterials. 24 (2003) 3955-3968.
25. Ferracane, J.L., *Hygroscopic and hydrolytic effects in dental polymer networks.* Dent Mater. 22 (2006) 211-22.
26. Willems, G., P. Lambrechts, M. Braem, J.P. Celis and G. Vanherle, *A classification of dental composites according to their morphological and mechanical characteristics.* Dent Mater. 8 (1992) 310-9.
27. Beun, S., T. Glorieux, J. Devaux, J. Vreven and G. Leloup, *Characterization of nanofilled compared to universal and microfilled composites.* Dent Mater. 23 (2007) 51-9.
28. Sideridou, I.D., M.M. Karabela and E. Vouvoudi, *Physical properties of current dental nanohybrid and nanofill light-cured resin composites.* Dent Mater. 27 (2011) 598-607.
29. Rodríguez, H.A., L.F. Giraldo and H. Casanova, *Formation of functionalized nanoclusters by solvent evaporation and their effect on the physicochemical properties of dental composite resins.* Dent Mater. 31 (2015) 789-798.
30. Asmussen, E. and A. Peutzfeldt, *Class I and Class II restorations of resin composite: An FE analysis of the influence of modulus of elasticity on stresses generated by occlusal loading.* Dent Mater. 24 (2008) 600-605.

31. Tanimoto, Y., T. Kitagawa, M. Aida and N. Nishiyama, *Experimental and computational approach for evaluating the mechanical characteristics of dental composite resins with various filler sizes.* Acta Biomater. 2 (2006) 633-9.
32. Leprince, J.G., W.M. Palin, M.A. Hadis, J. Devaux and G. Leloup, *Progress in dimethacrylate-based dental composite technology and curing efficiency.* Dent Mater. 29 (2013) 139-56.
33. Musanje, L. and B.W. Darvell, *Aspects of water sorption from the air, water and artificial saliva in resin composite restorative materials.* Dent Mater. 19 (2003) 414-22.
34. Ilie, N. and R. Hickel, *Macro-, micro- and nano-mechanical investigations on silorane and methacrylate-based composites.* Dent Mater. 25 (2009) 810-9.
35. Vouvoudi, E.C. and I.D. Sideridou, *Dynamic mechanical properties of dental nanofilled light-cured resin composites: Effect of food-simulating liquids.* J Mech Behav Biomed Mater. 10 (2012) 87-96.
36. Sideridou, I.D., E.C. Vouvoudi and E.A. Adamidou, *Dynamic mechanical thermal properties of the dental light-cured nanohybrid composite Kalore, GC: effect of various food/oral simulating liquids.* Dent Mater. 31 (2015) 154-61.
37. Halvorson, R.H., R.L. Erickson and C.L. Davidson, *Energy dependent polymerization of resin-based composite.* Dent Mater. 18 (2002) 463-9.
38. Truffier-Boutry, D., S. Demoustier-Champagne, J. Devaux, J.-J. Biebuyck, M. Mestdagh, P. Larbanois and G. Leloup, *A physico-chemical explanation of the post-polymerization shrinkage in dental resins.* Dent Mater. 22 (2006) 405-412.
39. Sideridou, I.D. and M.M. Karabela, *Sorption of water, ethanol or ethanol/water solutions by light-cured dental dimethacrylate resins.* Dent Mater. 27 (2011) 1003-10.
40. Manojlovic, D., M. Radisic, M. Lausevic, S. Zivkovic and V. Miletic, *Mathematical modeling of cross-linking monomer elution from resin-based dental composites.* J Biomed Mater Res B Appl Biomater. 101 (2013) 61-7.
41. Sideridou, I., V. Tserki and G. Papanastasiou, *Study of water sorption, solubility and modulus of elasticity of light-cured dimethacrylate-based dental resins.* Biomaterials. 24 (2003) 655-65.
42. Curtis, A.R., W.M. Palin, G.J. Fleming, A.C. Shortall and P.M. Marquis, *The mechanical properties of nanofilled resin-based composites: characterizing discrete filler particles and agglomerates using a micromanipulation technique.* Dent Mater. 25 (2009) 180-7.
43. Can Say, E., H. Yurdaguven, B.C. Yaman and F. Ozer, *Surface roughness and morphology of resin composites polished with two-step polishing systems.* Dent Mater J. 33 (2014) 332-42.
44. Yamasaki, L.C., A.G. De Vito Moraes, M. Barros, S. Lewis, C. Francci, J.W. Stansbury and C.S. Pfeifer, *Polymerization development of "low-shrink" resin composites: Reaction kinetics, polymerization stress and quality of network.* Dent Mater. 29 (2013) e169-79.
45. Blackham, J.T., K.S. Vandewalle and W. Lien, *Properties of hybrid resin composite systems containing prepolymerized filler particles.* Oper Dent. 34 (2009) 697-702.
46. Klapdohr, S. and N. Moszner, *New Inorganic Components for Dental Filling Composites.* Monatshefte für Chemie / Chemical Monthly. 136 (2004) 21-45.

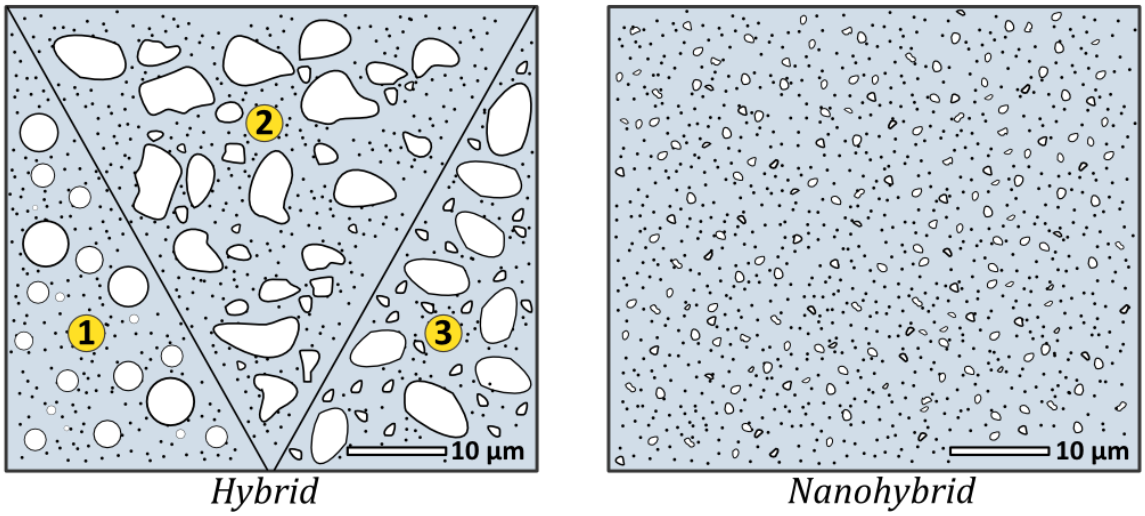

Figure 1: Schematic description of filler distribution according to current classification. Hybrid resin composites include a combination of micro and nanoparticles (left figure). Numbers denote continuous distributions (1 and 2) with spherical (1) or irregular particles (2) and a bimodal distribution (3) of micro particles. A nanohybrid resin composite contains nanoparticles (< 100 nm) and sub-micron "microparticles" (≤ 1 µm) (right figure)

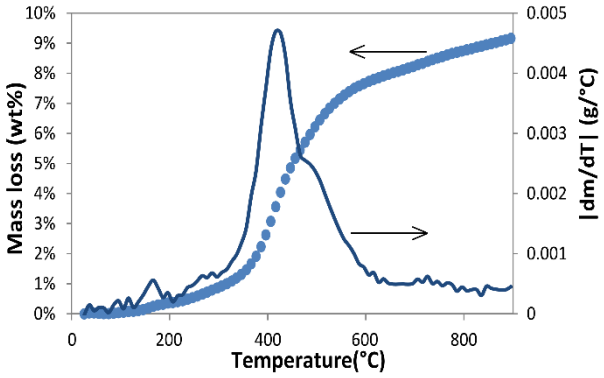

Figure 2: Mass loss (left axis) and its first derivative with respect to temperature (right axis) as a function of temperature, measured with TGA for Aerosil R7200 (methacrylsilane aftertreated fumed silica, Evonik GmbH)

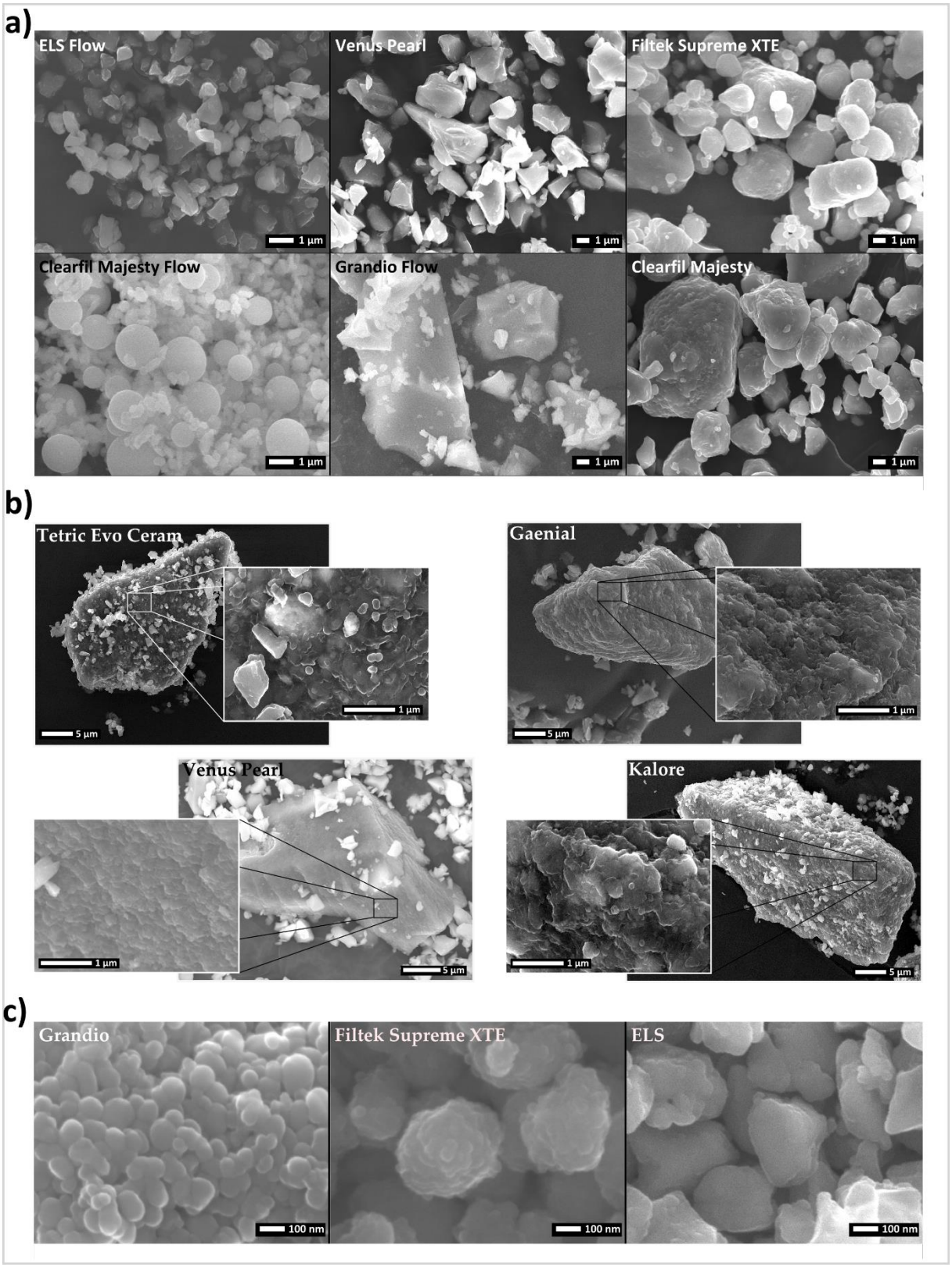

Figure 3: a) representative SEM pictures showing the variation in size and geometry for a selection of "micro" particles. Scale bar is 1 µm in the six pictures (5 000 or 10 000 x magnification). b) representative SEM pictures showing the size and geometry of some pre-

polymerized fillers found in *Tetric Evo Ceram*, *Gaenial*, *Venus Pearl* and *Kalore*. The scale bar in the three inserts is identical (30 000x magnification). c) representative SEM pictures showing the variation in geometry for a selection of "nano" particles. Scale bar is 100 nm in the three pictures (100 000 x magnification)

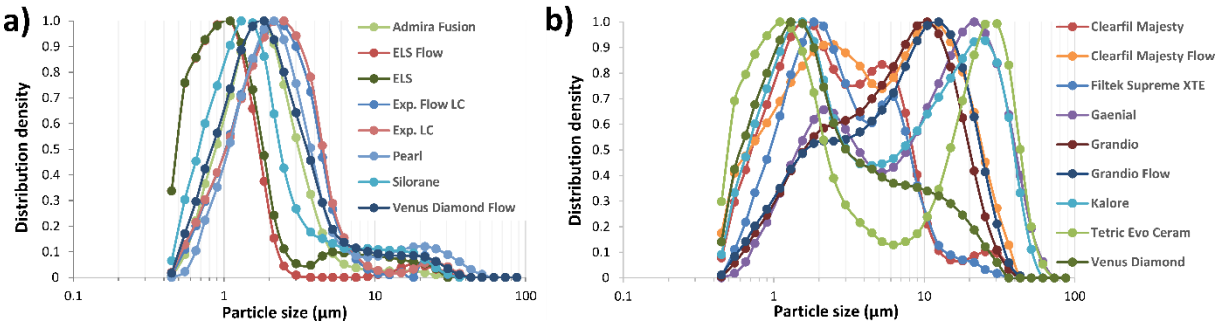

Figure 4: Particle density distribution, plotted as a function of the estimated particle size extracted by sedimentation during the first cycle (micro particles). Materials were grouped based on unimodal (a) or bimodal (b) distributions. In a), the bumps seen around 10 µm correspond to aggregated particles

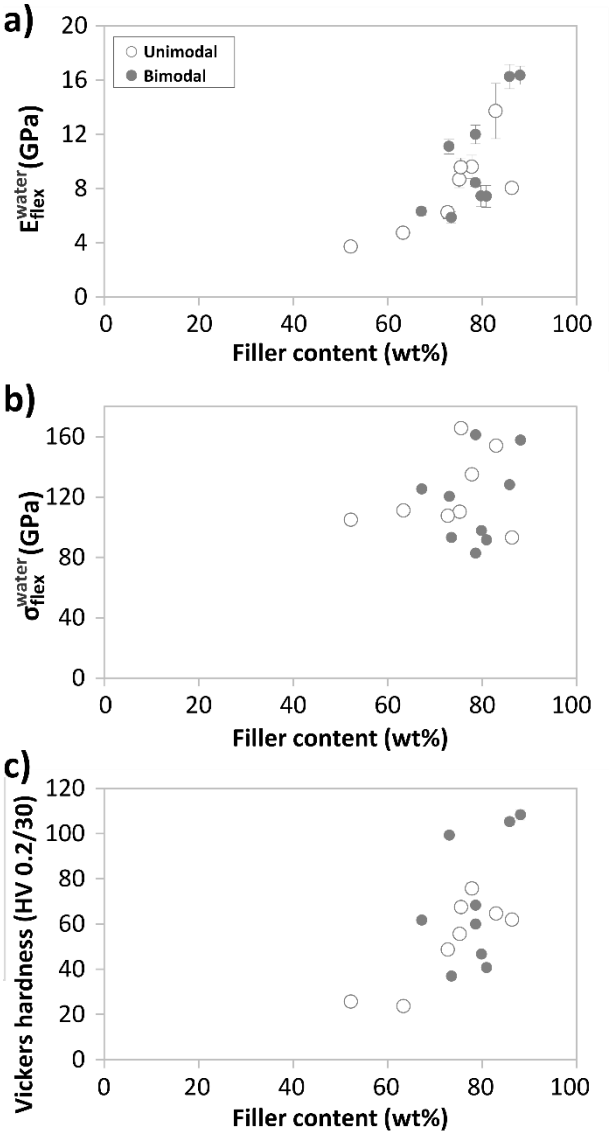

Figure 5: Flexural modulus, flexural strength and Vickers hardness (a, b and c, respectively) plotted as a function of the highest filler content measured either by centrifugation or TGA. Data includes all materials tested after an aqueous incubation of 1 week at 37 °C. Error bars indicate standard deviations and may be hidden by symbols or were excluded for clarity (in b)

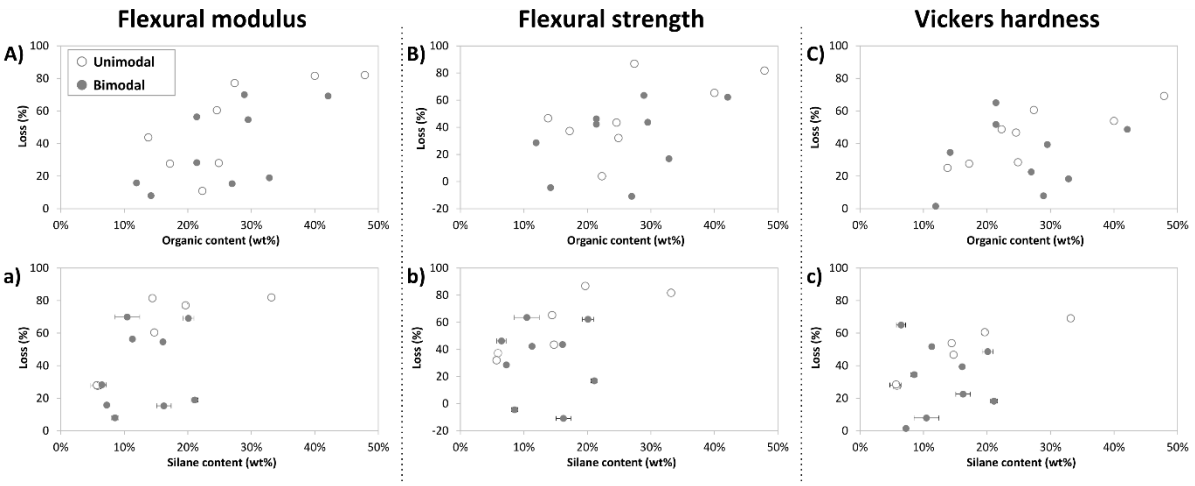

Figure 6: flexural modulus, flexural strength and hardness losses after an ethanol/water incubation compared to water, as a function of organic content (A, B and C, respectively) or organic content (a, b and c, respectively). Average values for each material are shown and error bars indicate standard deviations. Error bars for the organic content are hidden by the symbols

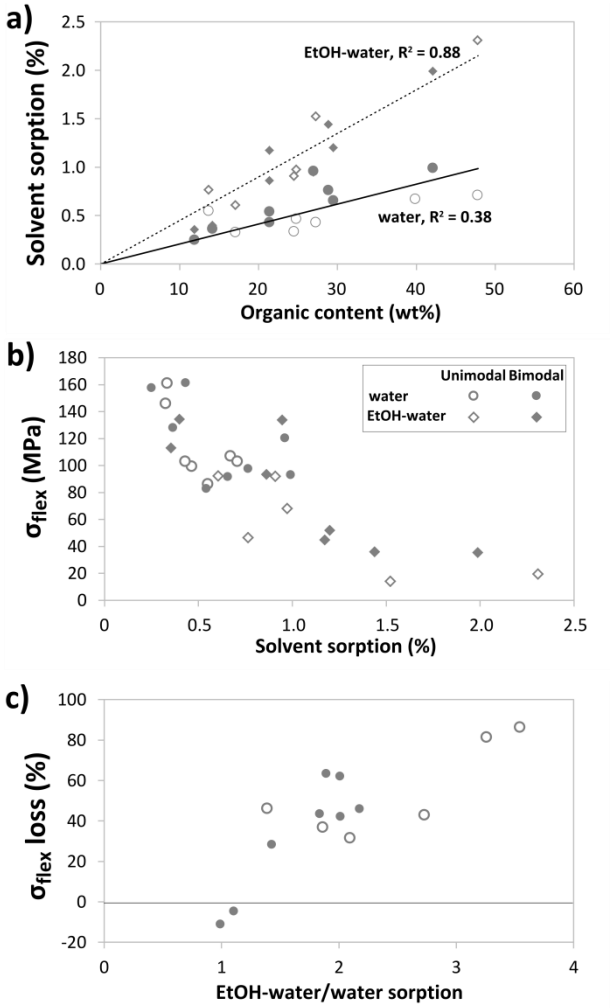

Figure 7: a) water (circles) or ethanol/water (diamonds) sorption as a function of organic content. Linear fits were applied to all data and constrained to pass through the origin point; b) Flexural strength as a solvent sorption; c) Loss in flexural strength between the ethanol/water and water incubation as a function of the ratio of solvent sorptions (only fourteen materials appear; for the *Filtek Silorane*, *Clearfil Majesty Flow* and *Venus Diamond Flow*, S or R could not be determined). In all graphs, average values for each material are shown and error bars were omitted

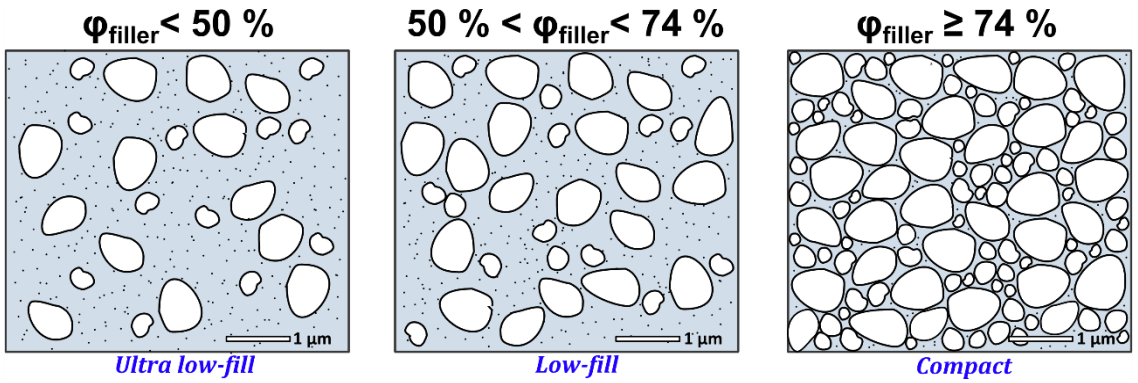

Figure 8: Simple classification based on the inorganic filler volume content, which would reflect the elastic modulus. A resin composite containing nano and micron-sized particles is presented

Tables

Table 1 Description of resin composites used in the study. Data provided by the manufacturers. PPF stands for Pre-Polymerized Fillers

Material/Shade	Type/Format	Batch n°	Organic matrix	Manufacturer
Admira Fusion/A3	Nanohydrid Ormocer/Composite	V53177	Ormocer	Voco GmbH
Clearfil Majesty ES Flow/A3	Nanohybrid/Flowable	1K0078		Kuraray Dental
Clearfil Majesty Posterior/A3	Nanohybrid/Composite	BC0013		Kuraray Dental
ELS Flow/A3op	Microhydrid/Flowable	B810	TegDMA & HEMA-free, Low-shrink	Saremco dental
ELS/A3	Microhydrid/Composite	B797	TegDMA & HEMA-free, Low-shrink	Saremco dental
Exp. Flow LC/A3	Experimental flowable	V55226		Voco GmbH
Exp. LC/A3	Experimental Composite	V53177		Voco GmbH
Filtek Silorane/A3	Microhybrid/Composite	N462672	Low-shrink	3M ESPE
Filtek Supreme XTE/A3	Nanohybrid/Composite	N609054		3M ESPE
Gaenial Anterior/A3	Nanohybrid/Composite	1311281	BisGMA-free, PPF	GC
Grandio Flow/A3	Nanohybrid/Flowable	1344366		Voco GmbH
Grandio/A3	Nanohybrid/Composite	1408240		Voco GmbH
Kalore/A3	Nanohydrid/Composite	1309051	Low-shrink, PPF	GC
Tetric Evo Ceram/A3	Nanohybrid/Composite	P11989	PPF	Ivoclar Vivadent
Venus Diamond Flow/A3	Nanohybrid/Flowable	010102		Heraeus Kulzer
Venus Diamond/A3	Nanohybrid/Composite	010052		Heraeus Kulzer
Venus Pearl/A3	Microhybrid/Composite	010029	PPF	Heraeus Kulzer

Table 1 bis Description of resin composites used in the study. Data and information collected from manufacturers' brochures and scientific product files

Material	Filler content wt%/vol%	Filler specifications
Admira Fusion	84/*NS*	
Clearfil Majesty Posterior	92/82	Glass ceramics/Alumina micro particles (0.02-7.9 µm)

Clearfil Majesty ES Flow	75/59	Barium glass/silica particles (0.18-3.5 µm)
ELS	74/49	Barium glass/silica particles (0.004-3 µm)
ELS Flow	53/28	Barium glass particles (0.05-3 µm)
Exp. Flow LC	*NS*	
Exp. LC	*NS*	
Filtek Silorane	76/55	Quartz and Yttrium fluoride particles
Filtek Supreme XTE	78.5/63.3	0.6-10 µm zirconia/silica clusters, 20 nm silica (20 nm) and zirconia (4-11 nm) dispersed particles
Gaenial Anterior		Two types of pre-polymerized particles ([400 nm Strontium glass and 100 nm lanthanoid fluoride] or [16 nm silica)]) (16-17 µm), silica (850 nm) and fumed silica (16 nm)
Grandio	87.0/71.4	
Grandio Flow	80.2/65.7	
Kalore	82/*NS*	17 µm pre-polymerized particles (400 nm Strontium glass and 100 nm lanthanoid fluoride), Strontium and fluoroaluminosilicate glasses (700 nm), silica (16nm)
Tetric Evo Ceram	82.5/NS	34 wt% Pre-polymerized and 48.5 wt% Ytterbium fluoride, Barium glass and mixed oxide particles (0.4-0.7 µm)
Venus Diamond	81/64	Barium Aluminium Fluoride glass/highly discrete nanoparticles (5 nm-20 µm)
Venus Diamond Flow	65/41	Barium Aluminium Fluoride Silicate glass/Ytterbium Fluoride and Silicium Oxide (20 nm- 5 µm)
Venus Pearl	80/59	Barium Aluminium Fluoride glass /highly discrete nanoparticles (5 nm-5 µm)

Table 2 Density of the un-cured resin composites, filler contents quantified by TGA corresponding to total inorganic content (W_i) and by centrifugation corresponding to an acetone-insoluble fraction (W_{total}), itself resulting from the sum of contents of particles larger or smaller than ≈ 500 nm ($W_{>500}$ or $W_{<500}$ respectively). Standard deviations of three measurements in parentheses. * a significant fraction of the smallest particles was not recovered

Material	**d (g/cm^3)**	W_i **(wt%)**	W_{total} **(wt%)** =	$W_{>500}$ **(wt%)** +	$W_{<500}$ **(wt%)**
Admira Fusion	2.18	86.3 (0.2)	78.1 (0.9)	61.7 (0.6)	16.4 (0.5)*
Clearfil Majesty ES Flow	1.80	67.2 (0.1)	66.9 (0.1)	25.5 (0.4)	41.4 (0.4)
Clearfil Majesty Posterior	2.39	88.1 (0.1)	78.9 (0.5)	69.8 (0.2)	9.1 (0.3)*
ELS	2.07	72.7 (0.1)	72.1 (0.6)	59.1 (0.3)	13.0 (0.4)
ELS Flow	1.68	52.2 (0.1)	52.1 (0.1)	43.5 (0.1)	8.6 (0.1)
Exp. Flow LC	1.91	75.2 (0.3)	72.0 (0.9)	59.8 (0.6)	12.2 (0.4)

Exp. LC	2.10	82.9 (0.1)	79.6 (0.1)	67.3 (0.1)	12.3 (0.1)
Filtek Silorane	2.02	77.8 (0.1)	74.2 (1.1)	62.4 (0.9)	11.8 (1.1)
Filtek Supreme XTE	1.90	73.0 (0.2)	64.9 (0.5)	58.8 (0.3)	6.1 (0.4)*
Gaenial	1.72	57.8 (0.1)	73.5 (0.1)	68.2 (0.2)	5.2 (0.1)
Grandio	2.06	85.8 (0.3)	83.2 (1.3)	73.6 (1.2)	9.6 (0.1)
Grandio Flow	1.91	78.6 (0.2)	76.1 (0.9)	64.0 (0.7)	12.1 (0.3)
Kalore	1.97	71.1 (0.1)	79.8 (0.6)	74.0 (1.8)	5.8 (1.2)
Tetric Evo Ceram	2.18	70.5 (0.1)	80.9 (0.3)	65.9 (0.9)	15.0 (0.6)
Venus Diamond	2.20	78.6 (0.5)	76.4 (0.9)	68.4 (2.2)	8.1 (1.4)
Venus Diamond Flow	1.92	60.1 (0.1)	63.3 (0.2)	62.6 (0.1)	0.7 (0.2)
Venus Pearl	2.02	75.5 (0.1)	74.7 (1.5)	68.5 (0.3)	6.2 (1.7)

Table 3 Distribution characteristics. The subscript indicate the particle diameter at said % in the cumulative distribution

Material	d_{50} (µm)	d_{90} (µm)	d_{99} (µm)
Admira Fusion	1.6	3.3	13.2
Clearfil Majesty ES Flow	3.6	16.6	29.4
Clearfil Majesty Posterior	2.1	7.2	26.2
ELS	0.8	3.2	19.2
ELS Flow	0.8	1.6	17.4
Exp. Flow LC	2.0	4.2	18.6
Exp. LC	2.0	4.3	23.1
Filtek Silorane	1.3	6.0	21.3
Filtek Supreme XTE	2.3	7.2	18.0
Gaenial	8.2	28.3	45.5
Grandio	5.6	15.6	26.1
Grandio Flow	6.1	17.5	29.3
Kalore	4.6	26.0	42.1
Tetric Evo Ceram	1.8	30.0	46.7
Venus Diamond	1.7	11.3	24.2
Venus Diamond Flow	1.6	3.9	14.7
Venus Pearl	2.0	8.7	32.3

Table 4 Mechanical properties of the tested resin composites. Standard deviations in parentheses. Letters connect similar values in each column ($p < 0.05$)

Material	**water**			**75/25 vol% ethanol/water**		
	E_{flex} **(GPa)**	**σ (MPa)**	**HV 0.2/30**	E_{flex} **(GPa)**	**σ (MPa)**	**HV 0.2/30**
Admira Fusion	8.0 (0.4) ^{F,G}	86 (18) ^{F,G}	62.0 (1.0) ^{G}	4.6 (0.3) ^{H}	46 (10) ^{F,G}	46.7 (0.6) ^{E}
Clearfil Majesty ES Flow	6.3 (0.3) ^{H,I}	126 (10) ^{B,C,D}	61.7 (1.7) ^{G,H}	5.1 (0.3) ^{G}	105 (15) ^{C}	50.3 (0.6) ^{D}
Clearfil Majesty Posterior	16.3 (0.7) ^{A}	158 (19) ^{A}	108.3 (2.3) ^{A}	13.8 (0.7) ^{B}	113 (14) ^{C}	106.7 (1.2) ^{A}
ELS	6.2 (0.4) ^{I}	103 (11) ^{D,E,F,G}	48.7 (0.6) ^{J}	1.4 (0.1) ^{K}	14 (3) ^{J}	19.3 (0.6) ^{L}
ELS Flow	3.7 (0.1) ^{J}	103 (5) ^{D,E,F,G}	25.7 (0.6) ^{N}	0.7 (0.1) ^{L}	19 (2) ^{J}	8.0 (0.2) ^{N}
Exp. Flow LC	8.7 (0.6) ^{D,E,F}	100 (33) ^{E,F,G}	55.7 (1.2) ^{I}	6.3 (0.3) ^{F}	68 (14) ^{E}	40.0 (0.8) ^{G}
Exp. LC	13.7 (2.0) ^{B}	146 (20) ^{A,B}	64.7 (0.5) ^{F}	10.0 (1.1) ^{C}	92 (14) ^{D}	47.0 (0.4) ^{E}
Filtek Silorane	9.6 (0.8) ^{D}	128 (12) ^{B,C}	55.7 (1.2) ^{D}	8.6 (0.8) ^{E}	124 (18) ^{B}	39.1 (0.5) ^{G}
Filtek Supreme XTE	11.1 (0.6) ^{C}	120 (9) ^{C,D,E}	99.2 (1.3) ^{C}	9.4 (0.3) ^{D}	134 (9) ^{A}	77.0 (0.5) ^{B}
Gaenial	5.9 (0.4) ^{I}	93 (6) ^{F,G}	37.0 (0.0) ^{M}	1.8 (0.1) ^{J,K}	35 (3) ^{I}	19.1 (0.4) ^{L}
Grandio	16.3 (0.9) ^{A}	128 (18) ^{B,C}	105.3 (1.5) ^{B}	15.0 (0.8) ^{A}	134 (12) ^{A}	69.0 (1.0) ^{C}
Grandio Flow	8.4 (0.3) ^{E,F,G}	83 (10) ^{G}	60.0 (0.0) ^{H}	6.1 (0.5) ^{F}	38 (8) ^{F,G,H}	21.0 (0.6) ^{K}
Kalore	7.5 (0.3) ^{G,H}	98 (4) ^{E,F,G}	46.7 (0.6) ^{K}	2.2 (0.1) ^{J}	36 (2) ^{H,I}	43.0 (0.5) ^{F}
Tetric Evo Ceram	7.4 (0.3) ^{G,H}	92 (4) ^{F,G}	40.7 (1.3) ^{L}	3.4 (0.3) ^{I}	52 (7) ^{F}	24.7 (1.2) ^{J}
Venus Diamond	12.0 (0.7) ^{C}	161 (14) ^{A}	68.3 (0.6) ^{E}	5.2 (0.4) ^{G}	93 (10) ^{D}	33.0 (0.1) ^{I}

Venus Diamond Flow	4.7 (0.2) [J]	107 (10) [C,D,E,F]	23.7 (0.4) [O]	0.9 (0.1) [L]	38 (4) [G,H,I]	11.0 (0.1) [M]
Venus Pearl	9.6 (0.7) [D,E]	161 (12) [A]	67.5 (0.9) [E]	3.8 (0.5) [I]	92 (12) [D]	36.4 (1.5) [H]

Table 5 Degradation of the mechanical properties after an incubation in 75/25 vol% ethanol/water compared to water (both 1 week at 37 °C)

Material	E_{flex} **(%)**	**σ (%)**	**HV (%)**
Admira Fusion	43	46	25
Clearfil Majesty ES Flow	19	-18	18
Clearfil Majesty Posterior	16	28	2
ELS	77	86	60
ELS Flow	82	81	69
Exp. Flow LC	28	34	28
Exp. LC	27	36	27
Filtek Silorane	11	3	49
Filtek Supreme XTE	15	-10	23
Gaenial	69	62	49
Grandio	8	-2	35
Grandio Flow	28	45	65
Kalore	70	63	8
Tetric Evo Ceram	55	42	39
Venus Diamond	56	42	52
Venus Diamond Flow	81	65	54
Venus Pearl	60	42	46

Table 6 Sorption (S) and released matter (R) after one week of incubation at 37 °C in either water or ethanol/water. Standard deviations in parentheses. *x* indicate that due to significant solvent retention, no value could be determined

Material	S_{water} **(%)**	$S_{ethanol/water}$ **(%)**	R_{water} **(%)**	$R_{ethanol/water}$ **(%)**
Admira Fusion	0.55 (0.01)	0.76 (0.02)	0.12 (0.07)	0.07 (0.02)
Clearfil Majesty ES Flow	*x*			
Clearfil Majesty Posterior	0.25 (0.00)	0.35 (0.02)	0.02 (0.01)	0.20 (0.02)
ELS	0.43 (0.02)	1.52 (0.09)	0.09 (0.01)	0.89 (0.02)
ELS Flow	0.71 (0.02)	2.31 (0.22)	0.11 (0.04)	0.74 (0.18)
Exp. Flow LC	0.46 (0.06)	0.97 (0.15)	0.11 (0.01)	0.37 (0.01)
Exp. LC	0.33 (0.01)	0.61 (0.02)	0.10 (0.02)	0.32 (0.01)
Filtek Silorane	*x*			
Filtek Supreme XTE	0.96 (0.01)	0.95 (0.05)	0.09 (0.01)	0.20 (0.01)
Gaenial	0.99 (0.01)	1.99 (0.05)	0.06 (0.04)	0.48 (0.04)
Grandio	0.36 (0.02)	0.40 (0.00)	0.09 (0.09)	0.14 (0.01)
Grandio Flow	0.54 (0.01)	1.17 (0.06)	0.28 (0.02)	0.75 (0.08)
Kalore	0.76 (0.03)	1.44 (0.13)	0.09 (0.05)	0.44 (0.09)
Tetric Evo Ceram	0.65 (0.08)	1.20 (0.18)	0.15 (0.09)	0.56 (0.14)
Venus Diamond	0.43 (0.01)	0.86 (0.03)	0.13 (0.00)	0.44 (0.03)
Venus Diamond Flow	*x*			
Venus Pearl	0.33 (0.01)	0.91 (0.02)	0.02 (0.00)	0.42 (0.02)